

Figure 9 Main axis direction of the antenna; axial ratio is also plotted

coefficients that were calculated from the corresponding axial ratio and main axis angle. From these measurements, the circular polarization gain was calculated for both right-hand circular polarization (RHCP) and left-hand circular polarization (LHCP). Both the RHCP and LHCP gains are presented in Figure 10. The RHCP gain is dominant within the operating bandwidth, and the RHCP and LHCP gains are similar outside the frequency band since there the antenna predominantly radiates a linearly polarized EM wave.

5. CONCLUSIONS

In this paper, a fast and rigorous synthesis method of a circularly polarized microstrip stacked patch antenna is proposed. The CPU time efficiency is increased on both the electromagnetic simulator side and the optimization side of the procedure. On the electromagnetic simulator side, patch currents are calculated using entire-domain basis and test functions in the MoM in the spectral domain. A small number of basis and test functions enabled a fast, but still rigorous calculation of the cost function related to antenna performance. On the optimization side of the problem, the CPU-time efficiency is increased by using a hybrid genetic algorithm that consists of the genetic algorithm (for reliable global search) and the direct search routine to overcome the slow convergence of the common GA in late generations. Analysis of the hybrid GA showed the capability for signifi-

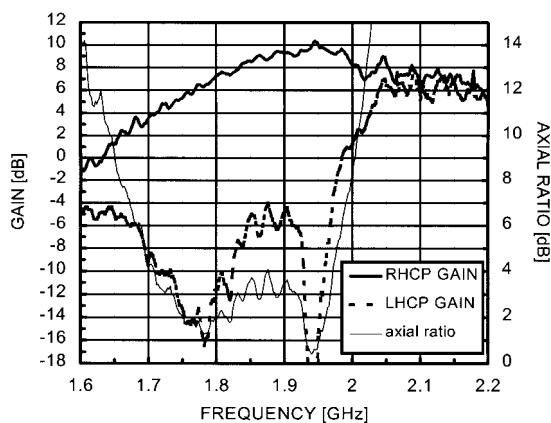


Figure 10 RHCP and LHCP gain of the antenna; axial ratio is also plotted to mark the operating bandwidth

cant acceleration of the optimization scheme. The whole procedure was tested on a problem of stacked patches for circular polarization in the 1800/1900 MHz band. The optimal antenna was built and measured. The realized antenna was well matched ($SWR < 2$), with an axial ratio lower than 4 dB within a 14% bandwidth.

REFERENCES

1. N. Herscovici, Z. Sipus, and D. Bonafacic, Circularly polarized single-fed wide band microstrip elements and arrays, 1999 IEEE AP-S Conf Antennas Propagat, Orlando, FL, 1999, pp. 280–283.
2. N. Herscovici, Z. Sipus, and D. Bonafacic, Circularly polarized single-fed microstrip patch for wireless communications, Proc 1998 IEEE AP-S Conf Antennas Propagat for Wireless Commun, Waltham, MA, Oct. 1998, pp. 167–170.
3. R. Zentner, Z. Sipus, and J. Bartolic, Synthesis of broadband microstrip antennas, Proc AP2000 Millennium Conf Antennas Propagat, Davos, Switzerland, Apr. 2000, pp. p0939/1p0939/4.
4. D.M. Pozar, Input impedance and mutual coupling of rectangular microstrip antennas, IEEE Trans Antennas Propagat AP-30 (1982), 1191–1196.
5. Z. Sipus, P.-S. Kildal, R. Leijon, and M. Johansson, An algorithm for calculating spectral domain Green's functions for planar, circular cylindrical and spherical multilayer structures, ACES J 13 (1998), 243–254.
6. L. Davis (Editor), Handbook of genetic algorithms, Van Nostrand Reinhold, New York, 1991.
7. D.E. Goldberg, Genetic algorithms in search, optimization and machine learning, Addison-Wesley, Reading, MA, 1989.
8. K.-K. Yan and Y. Lu, Sidelobe reduction in array-pattern synthesis using genetic algorithm, IEEE Trans Antennas Propagat 45 (1997), 1117–1121.
9. Y.H. Lee, A.C. Marvin, and S.J. Potter, Genetic algorithms using real parameters for efficient antenna design optimisation, Proc AP2000 Millennium Conf Antennas Propagat, Davos, Switzerland, Apr. 2000, pp. p0621/1–p0621/4.
10. W.H. Press, S.A. Teukolsky, W.T. Vetterling, and B.P. Flannery, Numerical recipes (in Fortran), The art of scientific computing, Cambridge University Press, Cambridge, England, 1994, 2nd ed.

© 2001 John Wiley & Sons, Inc.

MODELING OF MULTIPLE SCATTERING AMONG VIAS IN PLANAR WAVEGUIDES USING FOLDY-LAX EQUATIONS

Leung Tsang,¹ Houfei Chen,¹ Chung-Chi Huang,¹ and Vikram Jandhyala¹

¹Department of Electrical Engineering
University of Washington
Seattle, Washington 98195

Received 23 May 2001; revised 5 July 2001

ABSTRACT: The full-wave solution of multiple scattering among cylindrical vias in planar waveguides is modeled by using Foldy-Lax equations. By using the equivalence principle, the coupling among traces with

Contract grant sponsor: Washington Technology Center

Contract grant sponsor: HyperLynx

Contract grant sponsor: Intel Corporation

many vias is decomposed into interior and exterior problems. For the interior problem, the dyadic Green's function is expressed in terms of vector cylindrical waves and waveguide modes. The Foldy-Lax equations of multiple scattering among the cylindrical vias are calculated. The waveguide modes are decoupled in the Foldy-Lax equations. The scattering matrix of coupling among vias is calculated. Numerical simulations of the scattering matrix are illustrated for several hundred vias. © 2001 John Wiley & Sons, Inc. Microwave Opt Technol Lett 31: 201-208, 2001.

Key words: vias; vector cylindrical waves; Foldy-Lax equation; multiple scattering

1. INTRODUCTION

Via structures are predominantly used in multilayered packages to connect together traces residing in/on different layers. These are used extensively primarily because of high speeds, densities, and routing complexity. Parallel-plate waveguide effects are induced by the multilayered geometry; signals on active vias can excite waveguide modes within layers, and hence can affect other separated vias; the affected vias can, in turn, influence the original signal. Because of the waveguide modes, such coupling is not necessarily localized in space. This poses considerable design problems for reliability, high speed, and simulation. Such coupling can even cause unreliable behavior or complete signal failure, along with signal integrity loss, higher delays, and inappropriate switching of signals.

Classes of methods have been developed that aim to model the crosstalk or coupling mechanism through equivalent circuits. For instance, lumped inductance or capacitance models are developed [1]. These models only function well at very low frequencies. In particular, propagation and high-frequency scattering effects are not modeled accurately.

High-accuracy numerical techniques have also been developed to address this problem. The method of moments (MoM) is an integral-equation method formulated in the frequency domain [2, 3], while the finite-difference time-domain (FDTD) method is a differential equation method in the time domain [4]. Both of these methods can be used to theoretically solve the coupling problem accurately. These techniques have large computational time and memory overheads, and thus, in practice, have been used to model only small sections of the complete package structure.

A semianalytical approach attempt to account for coupling noise between coupled vias is shown by Gu et al. in [5, 6]. Coupling between two adjacent vias was analyzed using equivalent magnetic frill array models and a capacitor plate antenna based on Otto's approach [7]. These models were combined with even- odd-mode decomposition. This method assumes symmetry of the two vias, and neglects the influence of other vias. In reality, it is necessary to model large-scale distributed coupling effects due to large-scale mode coupling and crosstalk.

In this paper, we use a semianalytical technique of Foldy-Lax equations [8] to compute the full-wave solution of multiple scattering cylindrical vias in planar waveguides. By using the equivalence principle, the coupling among traces with many vias is decomposed into interior and exterior problems. For the interior problem, the dyadic Green's function is expressed in terms of vector cylindrical waves and waveguide modes. The Foldy-Lax equations of multiple scattering [8-10] among the cylindrical vias are derived. The waveguide modes are decoupled in the Foldy-Lax equations

so that the solution can be calculated for each waveguide mode separately. By combining with the exterior problem of signal traces, the scattering matrix of coupling many vias is derived. The results greatly simplify if the vias are of small radius and the waveguide thickness is small. For the case of coupled vias, the results compare well with that of Gu et al. [6]. We also illustrate the scattering matrix for several hundred vias.

2. EXTERIOR PROBLEM AND INTERIOR PROBLEM

Consider the problem of traces connected to vias. The vias pass through apertures in the ground planes and the power planes (Fig. 1). The two planes will form a parallel-plate waveguide. By using the equivalence principle, the apertures can be replaced by a perfect electric conductor, with equal and opposite magnetic currents on the two sides of the apertures. Thus, we will have the exterior problem of traces with magnetic surface current as indicated (Fig. 2). We also have the interior problem with magnetic surface currents as indicated (Fig. 3). With the apertures replaced by PECs, we have a parallel-plate waveguide with cylindrical vias. The exterior problem and the interior problem can be solved separately. After the solutions of the exterior and interior problems are computed, the two results are related by imposing the condition of equal and opposite magnetic currents. We also have the continuity of electric currents at the aperture between the interior and exterior problems (Fig. 4).

3. CYLINDRICAL-WAVE EXPANSION OF DYADIC GREEN'S FUNCTION IN PARALLEL WAVEGUIDE MODES

Consider two perfect electric conductors at $z = d/2$ and $z = -d/2$. In the multivias problem, the equivalence principle will be invoked with equivalent magnetic sources at $z' = \pm d/2$. Consider the general case of the magnetic source z' between the two PECs (Fig. 3). We use the dyadic Green's function to represent the magnetic field. The primary Green's function $\overline{\overline{G}}_p$ is the direct wave from the source with multiple reflections by the parallel plates. The solution is expressed in terms of waveguide modes, and also in terms of vector cylindrical waves for adapting to via scattering later. Notations are based on [9] and [10], with $\exp(-i\omega t)$ dependence

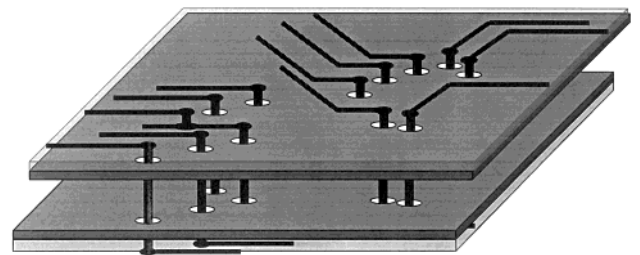


Figure 1 3-D view of massively coupled vertical vias connected to traces in layered geometry

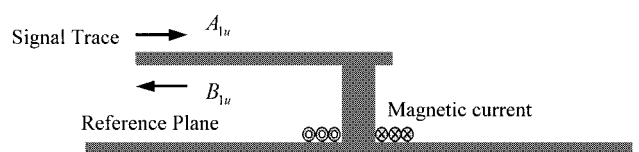


Figure 2 Exterior structure with aperture replaced by PEC with equivalent magnetic current

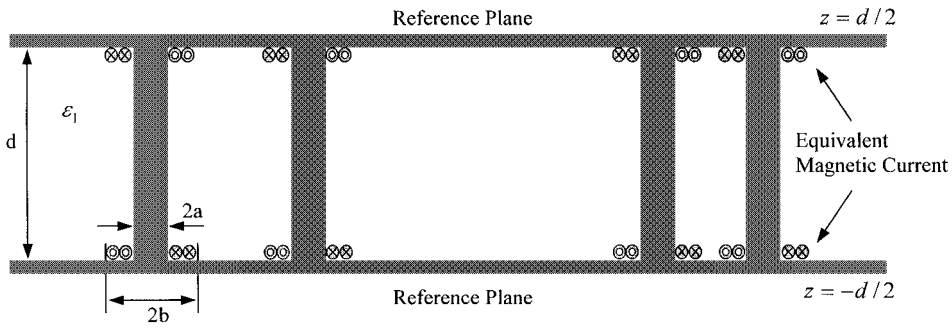


Figure 3 Interior structure with aperture replaced by PEC with equivalent magnetic current

in the two references changed to $\exp(j\omega t)$ dependence here. Let $\bar{\bar{I}}_t = \hat{x}\hat{x} + \hat{y}\hat{y}$ be the transverse dyad. Then

$$\bar{H} = -j\omega\epsilon \iint dx' dy' \bar{\bar{G}}(\bar{r}, \bar{r}') \cdot \bar{M}_s(\bar{r}') \quad (1)$$

where $\bar{\bar{G}}$ is the dyadic Green's function and \bar{M}_s is the magnetic surface current.

The model solutions are

$$k_{z,l} = \frac{l\pi}{d} \quad (2)$$

with $l = 0, 1, 2, \dots$ for TM modes and $l = 1, 2, \dots$ for TE modes.

We define magnetic TE and TM modal solutions as follows:

$$\begin{aligned} Rg\bar{H}_n^{\text{TE}}(k_\rho, k_z, \bar{\rho}, z) &= \frac{e^{-jn\phi}}{\eta} \left\{ -\hat{\rho} \frac{jk_\rho k_z}{k} J'_n(k_\rho \rho) \cos(k_z z) \right. \\ &\quad \left. - \hat{\phi} \frac{nk_z}{k\rho} J_n(k_\rho \rho) \cos(k_z z) - \hat{z} \frac{k_\rho^2}{k} J_n(k_\rho \rho) j \sin(k_z z) \right\} \quad (3) \end{aligned}$$

$$\begin{aligned} Rg\bar{H}_n^{\text{TM}}(k_\rho, k_z, \bar{\rho}, z) &= \frac{j}{\eta} \left\{ -\hat{\rho} \frac{jn}{\rho} J_n(k_\rho \rho) - \hat{\phi} k_\rho J'_n(k_\rho \rho) \right\} e^{-jn\phi} \cos(k_z z) \quad (4) \end{aligned}$$

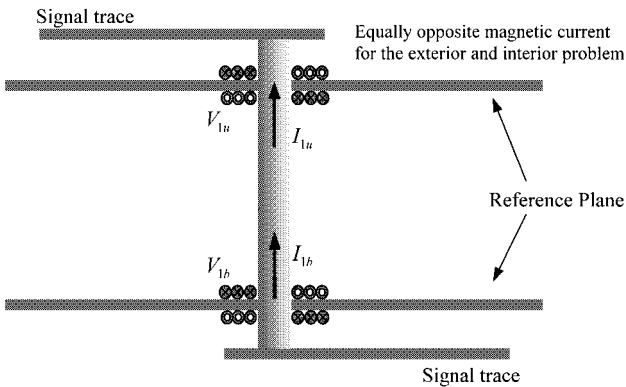


Figure 4 Voltages and currents of the exterior and interior problem: same notation for all traces and vias

where Rg stands for regular, with Bessel functions being used. Without the Rg , the corresponding functions are Hankel functions of the second kind. Also, $k_\rho = \sqrt{k^2 - k_z^2}$. The two vector cylindrical wave functions are

$$\bar{m}_n(k_\rho, k_z, \bar{\rho}) = -\hat{\rho} \frac{jn}{\rho} H_n^{(2)}(k_\rho \rho) - \hat{\phi} k_\rho H_n^{(2)'}(k_\rho \rho) \quad (5)$$

$$\begin{aligned} \bar{n}_n(k_\rho, k_z, \bar{\rho}) &= -\hat{\rho} \frac{jk_\rho k_z}{k} H_n^{(2)'}(k_\rho \rho) \\ &\quad - \hat{\phi} \frac{nk_z}{k\rho} H_n^{(2)}(k_\rho \rho) + \hat{z} \frac{k_\rho^2}{k} H_n^{(2)}(k_\rho \rho). \quad (6) \end{aligned}$$

In terms of the vector cylindrical waves expressed in modal solutions, the primary dyadic Green's functions are expressed below. We use the upper sign for $z > z'$ and the lower sign for $z < z'$.

For $\rho < \rho'$,

$$\begin{aligned} \bar{\bar{G}}_P(\bar{r}, \bar{r}') \cdot \bar{\bar{I}}_t &= -\frac{\eta}{4d} \sum_{n,l} \frac{(-1)^{n+l}}{k_{\rho l}^2} f_l (1 + e^{\mp 2jk_{z l}(z' \pm d/2)}) e^{\pm jk_{z l}(z' \pm d/2)} \\ &\quad \times Rg\bar{H}_n^{\text{TM}}(k_{\rho l}, k_{z l}, \bar{\rho}, z \mp d/2) \bar{m}_{-n}(k_{\rho l}, k_{z l}, \bar{\rho}') e^{jn\phi'} \cdot \bar{\bar{I}}_t \\ &\quad + \frac{j\eta}{4d} \sum_{n,l} \frac{(-1)^{n+l}}{k_{\rho l}^2} f_l (1 + e^{\mp 2jk_{z l}(z' \pm d/2)}) e^{\pm jk_{z l}(z' \pm d/2)} \\ &\quad \times Rg\bar{H}_n^{\text{TE}}(k_{\rho l}, k_{z l}, \bar{\rho}, z \mp d/2) \bar{n}_{-n}(k_{\rho l}, k_{z l}, \bar{\rho}') e^{jn\phi'} \cdot \bar{\bar{I}}_t \quad (7) \end{aligned}$$

and for $\rho > \rho'$,

$$\begin{aligned} \bar{\bar{G}}_P(\bar{r}, \bar{r}') \cdot \bar{\bar{I}}_t &= -\frac{\eta}{4d} \sum_{n,l} \frac{(-1)^{n+l}}{k_{\rho l}^2} f_l (1 + e^{\mp 2jk_{z l}(z' \pm d/2)}) e^{\pm jk_{z l}(z' \pm d/2)} \\ &\quad \times \bar{H}_n^{\text{TM}}(k_{\rho l}, k_{z l}, \bar{\rho}, z \mp d/2) Rg\bar{m}_{-n}(k_{\rho l}, k_{z l}, \bar{\rho}') e^{jn\phi'} \cdot \bar{\bar{I}}_t \\ &\quad + \frac{j\eta}{4d} \sum_{n,l} \frac{(-1)^{n+l}}{k_{\rho l}^2} f_l (1 + e^{\mp 2jk_{z l}(z' \pm d/2)}) e^{\pm jk_{z l}(z' \pm d/2)} \\ &\quad \times \bar{H}_n^{\text{TE}}(k_{\rho l}, k_{z l}, \bar{\rho}, z \mp d/2) Rg\bar{n}_{-n}(k_{\rho l}, k_{z l}, \bar{\rho}') e^{jn\phi'} \cdot \bar{\bar{I}}_t \quad (8) \end{aligned}$$

where

$$f_l = \frac{1}{2}, \quad \text{for } l = 0$$

$$= 1, \quad \text{for } l = 1, 2, \dots \quad (9)$$

4. FOLDY-LAX EQUATIONS FOR SCATTERING WITH MULTIPLE CYLINDERS

Consider N cylinders between the two parallel plates centered at $\bar{\rho}_1, \bar{\rho}_2 \dots \bar{\rho}_N$ and magnetic surface current density $\bar{M}_s = \bar{M}_{su}$ at $(\bar{\rho}', z' = d/2)$ and $\bar{M}_s = \bar{M}_{sb}$ at $(\bar{\rho}', z' = -d/2)$. The multiple scattering can be formulated in terms of Foldy-Lax multiple scattering equations. We use the upper sign for results with a source \bar{M}_{su} at $(\bar{\rho}', z' = d/2)$, and the lower sign for results with a source \bar{M}_{sb} at $(\bar{\rho}', z' = -d/2)$. The Foldy-Lax multiple scattering equations are formulated as follows. After multiple scattering, the final exciting field of cylinder p is

$$\bar{H}_{ex}^{(p)} = \sum_{n,l} w_{lm}^{\text{TM}(p)} \text{Rg} \bar{H}_m^{\text{TM}}(k_{\rho l}, k_{z l}, \bar{\rho} - \bar{\rho}_p, z \pm d/2)$$

$$+ \sum_{n,l} w_{lm}^{\text{TE}(p)} \text{Rg} \bar{H}_m^{\text{TE}}(k_{\rho l}, k_{z l}, \bar{\rho} - \bar{\rho}_p, z \pm d/2) \quad (10)$$

where $w_{lm}^{\text{TM}(p)}$ and $w_{lm}^{\text{TE}(p)}$ are exciting field coefficients to be solved by using the Foldy-Lax equations.

The T -matrix coefficients for perfect conducting cylinders are

$$T_n^{(M)} = T_{-n}^{(M)} = -\frac{J'_n(k_{\rho l} a)}{H_n^{(2)'}(k_{\rho l} a)} \quad (11)$$

$$T_n^{(N)} = T_{-n}^{(N)} = -\frac{J_n(k_{\rho l} a)}{H_n^{(2)}(k_{\rho l} a)}. \quad (12)$$

The Foldy-Lax equations state that the final exciting field of cylinder q is equal to the incident field plus scattered fields from all cylinders, except the scattered field from itself. The scattered field incident from cylinder p to cylinder q can be re-expressed by using the translation addition theorem for the modal solution \bar{H}_n^{TE} and \bar{H}_n^{TM} [10].

The Foldy-Lax multiple scattering equations are in the following form:

$$w_{ln}^{\text{TM}(q)} = a_{ln}^{\text{TM}(q)} + \sum_{\substack{p=1 \\ p \neq q}}^N \sum_{m=-\infty}^{\infty} H_{n-m}^{(2)}(k_{\rho l} |\bar{\rho}_p - \bar{\rho}_q|)$$

$$\times e^{j(n-m)\phi_{\bar{\rho}_p \bar{\rho}_q}} T_m^{(N)} w_{lm}^{\text{TM}(p)}$$

$$w_{ln}^{\text{TE}(q)} = a_{ln}^{\text{TE}(q)} + \sum_{\substack{p=1 \\ p \neq q}}^N \sum_{m=-\infty}^{\infty} H_{n-m}^{(2)}(k_{\rho l} |\bar{\rho}_p - \bar{\rho}_q|)$$

$$\times e^{j(n-m)\phi_{\bar{\rho}_p \bar{\rho}_q}} T_m^{(M)} w_{lm}^{\text{TE}(p)}$$

where $a_{ln}^{\text{TM}(q)}$, $a_{ln}^{\text{TE}(q)}$ are the incident fields of the current source onto cylinder q , and can be calculated by using the primary Green's function of the previous section. In the Foldy-Lax equations, there is no coupling between different l because each l corresponds to a specific k_z . Neither is there coupling between the TE and TM waves because the cylinders are perfectly conducting. Note that the primary Green's function is translationally invariant in the horizontal plane.

The incident field from the magnetic surface current source \bar{M}_s onto cylinder q is, using the translational addition theorem and translational invariance of $\bar{G}_p(\bar{r}, \bar{r}')$ in the horizontal direction,

$$-j\omega\epsilon \int d\bar{\rho}' \bar{G}_p(\bar{r}, \bar{r}') \cdot \bar{M}_s(\bar{\rho}')$$

$$= -j\omega\epsilon \int d\bar{\rho}' \bar{G}_p(\bar{\rho} - \bar{\rho}_q, z, \bar{\rho}' - \bar{\rho}_q, z') \cdot \bar{M}_s(\bar{\rho}'). \quad (13)$$

Using the expression of the primary dyadic Green's function from Eqs. (7) and (8) in the above, we calculate the incident field coefficients onto cylinder q :

$$a_{ln}^{\text{TM}(q)} = \frac{\eta j \omega \epsilon}{2d} \frac{(-1)^{n+1}}{k_{\rho l}^2} f_l \int d\bar{\rho}'$$

$$\times \bar{m}_{-n}(k_{\rho l}, k_{z l}, \bar{\rho}' - \bar{\rho}_q) e^{jn\phi_{\bar{\rho}' \bar{\rho}_q}} \cdot \bar{M}_s(\bar{\rho}') \quad (14)$$

$$= \frac{\eta \omega \epsilon}{2d} \frac{(-1)^{n+1}}{k_{\rho l}^2} f_l \int d\bar{\rho}'$$

$$\times \bar{n}_{-n}(k_{\rho l}, k_{z l}, \bar{\rho}' - \bar{\rho}_q) e^{jn\phi_{\bar{\rho}' \bar{\rho}_q}} \cdot \bar{M}_s(\bar{\rho}'). \quad (15)$$

After the Foldy-Lax multiple scattering equations are solved, the surface currents on the cylinder (p) are

$$\bar{J}_s^{(p)} = \sum_{m,l} w_{lm}^{\text{TM}(p)} \bar{J}_s^{\text{TM}}(k_{\rho l}, k_{z l}, z \pm d/2)$$

$$+ \sum_{m,l} w_{lm}^{\text{TE}(p)} \bar{J}_s^{\text{TE}}(k_{\rho l}, k_{z l}, z \pm d/2) \quad (16)$$

where the modal surface currents are

$$\bar{J}_{sn}^{\text{TE}}(k_{\rho}, k_z, z) = -\frac{(2j/\eta\pi k_{\rho} a) e^{-jn\phi}}{H_n^{(2)'}(k_{\rho} a)}$$

$$\times \left[-\hat{z} \frac{nk_z}{ka} \cos(k_z z) + \hat{\phi} \frac{k_{\rho}^2}{k} j \sin(k_z z) \right] \quad (17)$$

$$\bar{J}_{sn}^{\text{TM}}(k_{\rho}, k_z, z) = \hat{z} \frac{(2/\eta\pi a)}{H_n^{(2)}(k_{\rho} a)} \{\cos k_z z\} e^{-jn\phi}. \quad (18)$$

5. EXCITATION OF MAGNETIC FRILL CURRENT

Consider magnetic frill currents at aperture j with \bar{M}_{su} at $z' = d/2$ and \bar{M}_{sb} at $z' = -d/2$:

$$\bar{M}_{su}(\bar{\rho}') = -\frac{V_{ju}}{|\bar{\rho}' - \bar{\rho}_j| \ln(b/a)} \hat{\phi}_{\rho\rho_j}^+$$

$$\text{for } a \leq |\bar{\rho}' - \bar{\rho}_j| \leq b \quad (19)$$

$$\bar{M}_{sb}(\bar{\rho}') = -\frac{V_{jb}}{|\bar{\rho}' - \bar{\rho}_j| \ln(b/a)} \hat{\phi}_{\rho\rho_j}^+$$

$$\text{for } a \leq |\bar{\rho}' - \bar{\rho}_j| \leq b. \quad (20)$$

We first consider the excitation terms of $a_{ln}^{\text{TM}(j)}$ and $a_{ln}^{\text{TE}(j)}$ for cylinder j .

Because $\bar{n}_0(k_{\rho l}, k_{z l}, \bar{\rho}' - \bar{\rho}_j) = 0$,

$$a_{ln}^{\text{TM}(j)} = \frac{jk}{d} \frac{(-1)^l}{k_{\rho l}^2} f_l \frac{\pi V_j}{\ln(b/a)} \delta_{n0} [H_0^{(2)}(k_{\rho l} b) - H_0^{(2)}(k_{\rho l} a)] \quad (21)$$

$$a_{ln}^{\text{TE}(j)} = 0 \quad (22)$$

where $V_j = V_{ju}$ for \bar{M}_{su} and $V_j = V_{jb}$ for \bar{M}_{sb} .

Next, we calculate the excitation terms of $a_{ln}^{\text{TM}(q)}$ and $a_{ln}^{\text{TE}(q)}$ for cylinder $q \neq j$. We use the translation addition theorem since $|\bar{\rho}' - \bar{\rho}_q| < |\bar{\rho}_j - \bar{\rho}_q|$.

Thus, for $q \neq j$,

$$a_{ln}^{\text{TM}(q)} = \frac{jk}{2d} \frac{(-1)^{n+l}}{k_{\rho l}^2} f_l H_n^{(2)}(k_{\rho l} |\bar{\rho}_q - \bar{\rho}_j|) e^{jn\phi_{\rho_q} \theta_j} \times \left[\frac{2\pi V_j}{\ln(b/a)} [J_0(k_{\rho l} b) - J_0(k_{\rho l} a)] \right]. \quad (23)$$

After the exciting field coefficients are calculated, the surface current density on cylinder p is calculated from above. Then the current on cylinder (p) is

$$I^{(p)} = \int_0^{2\pi} ad\phi \bar{J}_s^{(p)} \cdot \hat{z} = 2\pi a \sum_l w_{l0}^{\text{TM}(p)}(\hat{z}) k_{\rho l} \frac{(2/\pi k_{\rho l} a)}{H_0^{(2)}(k_{\rho l} a)} \frac{1}{\eta} \{\cos k_{z l}(z \pm d/2)\}. \quad (24)$$

Next, we extend to the general case with N cylinders with voltages $V_{1u}, V_{2u}, \dots, V_{Nu}, V_{1b}, V_{2b}, \dots, V_{Nb}$ (Figs. 3 and 4). For sources at the upper aperture of $z' = d/2$, that is, $V_{1u}, V_{2u}, \dots, V_{Nu}$, the incident wave at cylinder q is

$$a_{ln}^{\text{TM}(q)} = \frac{jk}{2d} \frac{(-1)^{n+l}}{k_{\rho l}^2} f_l \frac{2\pi V_{qu}}{\ln(b/a)} \delta_{n0} \times [H_0^{(2)}(k_{\rho l} b) - H_0^{(2)}(k_{\rho l} a)] + \sum_{j \neq q}^N \frac{jk}{2d} \frac{(-1)^{n+l}}{k_{\rho l}^2} f_l H_n^{(2)}(k_{\rho l} |\bar{\rho}_q - \bar{\rho}_j|) e^{jn\phi_{\rho_q} \theta_j} \times \left[\frac{2\pi V_{ju}}{\ln(b/a)} [J_0(k_{\rho l} b) - J_0(k_{\rho l} a)] \right]. \quad (25)$$

We then solve the Foldy–Lax equations for $w_{ln}^{\text{TM}(q)}$. Then we find the currents at the cylinders at $z = +d/2$. That will be current I^{uu} , which is the current at $z = d/2$ due to the source at $z' = d/2$:

$$I^{(p)uu} = \sum_l w_{l0}^{\text{TM}(p)} \frac{4}{\eta H_0^{(2)}(k_{\rho l} a)} (-1)^l. \quad (26)$$

Then we find the currents at the cylinders at $z = -d/2$. That will be current I^{bu} , which is the current at $z = -d/2$ due to the source at $z' = d/2$:

$$I^{(p)bu} = \sum_l w_{l0}^{\text{TM}(p)} \frac{4}{\eta H_0^{(2)}(k_{\rho l} a)}. \quad (27)$$

Next, we consider the sources at the lower aperture of $-z' = d/2$, that is, V_{1b}, V_{2b}, \dots , and V_{Nb} . The Foldy–Lax equations are the same.

Then we find the currents at the cylinders at $z = +d/2$. That will be current I^{ub} , which is the current at $z = d/2$ due to the source at $z' = -d/2$.

We also find the currents at the cylinders at $z = -d/2$. That will be current I^{bb} , which is the current at the lower aperture $z = -d/2$ due to the sources of the lower aperture at $z' = -d/2$.

The total currents are

$$I^{(p)u} = I^{(p)uu} + I^{(p)ub} \quad (28)$$

$$I^{(p)b} = I^{(p)bu} + I^{(p)bb}. \quad (29)$$

6. MATRIX NOTATION FOR INTERIOR PROBLEM

Suppose that we have N vias, and we keep to $l = L_{\max}$ and multipoles up to $n = \pm N_{\max}$. Note that different l s are uncoupled. Then the dimension of \bar{w}_l is $M = N \times (2N_{\max} + 1)$, using a combined index of particle index $p = 1, 2, \dots, N$ and multipole index $n = -N_{\max}, -N_{\max} + 1, \dots, 0, 1, N_{\max}$. We can have a combined index of $\alpha = (q, n) = (2N_{\max} + 1) \times (q - 1) + n + N_{\max} + 1$. Thus, $\alpha = 1, 2, \dots, M$. Let superscript T denote the transpose of a matrix:

$$\bar{w}_l^T = \left[w_{l(-N_{\max})}^{(1)} \quad w_{l(-N_{\max}+1)}^{(1)} \quad \dots \quad w_{l(N_{\max})}^{(1)} \quad w_{l(-N_{\max})}^{(2)} \quad \dots \quad w_{l(N_{\max})}^{(2)} \quad \dots \quad w_{l(N_{\max})}^{(N)} \right]. \quad (30)$$

Thus, the dimension of the Foldy–Lax equations is M , and it is independent of the number of modes. That is, it is independent of the number of basis functions in the z -direction if modes are used. On the other hand, if N_z subsectional basis functions are used in the z -direction, then the dimension of the matrix equation is magnified N_z times. This decoupling drastically reduces the size of the matrix equation, particularly at high frequencies.

The Foldy–Lax matrix $\bar{\bar{F}}_l$ is of dimension $N(2N_{\max} + 1) \times N(2N_{\max} + 1) = M \times M$:

$$[\bar{\bar{F}}_l]_{qn, pm} = \delta_{nm} \delta_{qp} - (1 - \delta_{pq}) H_{n-m}^{(2)} \times (k_{\rho l} |\bar{\rho}_p - \bar{\rho}_q|) e^{j(n-m)\phi_{\bar{\rho}_p} \theta_q} T_m^{(N)}. \quad (31)$$

Define $\bar{\bar{E}}_l$ to be of dimension $M \times N$, so that

$$(\bar{\bar{E}}_l)_{qn, j} = [\bar{a}_{lj}]_{qn} \quad (32)$$

where

$$[\bar{a}_{lj}]_{qn} = \frac{jk}{2d} \frac{(-1)^l}{k_{\rho l}^2} f_l \frac{2\pi}{\ln(b/a)} \delta_{n0} \times [H_0^{(2)}(k_{\rho l} b) - H_0^{(2)}(k_{\rho l} a)], \quad \text{if } q = j$$

$$= \frac{jk}{2d} \frac{(-1)^{n+l}}{k_{\rho l}^2} f_l H_n^{(2)}(k_{\rho l} |\bar{\rho}_q - \bar{\rho}_j|) e^{jn\phi_{\rho_q} \theta_j} \frac{2\pi}{\ln(b/a)} \times [J_0(k_{\rho l} b) - J_0(k_{\rho l} a)], \quad \text{if } q \neq j. \quad (33)$$

Let voltage vectors \bar{V}^u be of dimension N , with $(\bar{V}^u)_j = V_{ju}$.

In matrix form, the Foldy–Lax equation is, for sources at $z' = d/2$,

$$\bar{F}_l \bar{w}_l^{(u)} = \bar{E}_l \bar{V}^u. \quad (34)$$

After the Foldy–Lax equation is solved, the currents can be computed. Let \bar{P}_l be of dimension $N \times N$:

$$(\bar{P}_l)_{p,j} = (\bar{F}_l^{-1} \bar{E}_l)_{p0,j}. \quad (35)$$

The $p0, j$ index is due to the fact that only the $n = 0$ th harmonic contributes to the current at the terminal, as indicated by Eq. (24). Next, we define current vectors of dimension N , \bar{I}^{uu} , which is the current at the upper aperture of $z = d/2$ due to the sources at $z' = d/2$. Also, define current vectors of dimension N , \bar{I}^{bu} , which is the current at the lower aperture of $z = -d/2$ due to the sources at $z' = d/2$:

$$\bar{I}^{uu} = \bar{Y}^{uu} \bar{V}^u \quad (36)$$

$$\bar{I}^{bu} = \bar{Y}^{bu} \bar{V}^u \quad (37)$$

where \bar{Y}^{uu} and \bar{Y}^{bu} are of dimension $N \times N$:

$$\bar{Y}^{uu} = \sum_l B_l \bar{P}_l \quad (38)$$

$$\bar{Y}^{bu} = \sum_l D_l \bar{P}_l \quad (39)$$

with

$$B_l = \frac{4(-1)^l}{\eta H_0^{(2)}(k_{\rho l} a)} \quad (40)$$

$$D_l = \frac{4}{\eta H_0^{(2)}(k_{\rho l} a)}. \quad (41)$$

Similarly, define current vectors of dimension N , \bar{I}^{ub} , which is the current at the upper aperture of $z = d/2$ due to the sources at $z' = -d/2$. Also, define current vectors of dimension N , \bar{I}^{bb} , which is the current at the lower aperture of $z = -d/2$ due to the sources at $z' = -d/2$.

Also, let voltage vectors \bar{V}^b be of dimension N . Then

$$\bar{I}^{ub} = \bar{Y}^{ub} \bar{V}^b \quad (42)$$

$$\bar{I}^{bb} = \bar{Y}^{bb} \bar{V}^b. \quad (43)$$

Because of reflection symmetry of the waveguide about $z = 0$, we have the symmetry relation of the admittance matrix elements $\bar{Y}^{ub} = \bar{Y}^{bu}$ and $\bar{Y}^{bb} = \bar{Y}^{uu}$.

After the interior problem is solved, the solution is represented by

$$\begin{bmatrix} \bar{I}^u \\ -\bar{I}^b \end{bmatrix} = -\bar{Y} \begin{bmatrix} -\bar{V}^u \\ \bar{V}^b \end{bmatrix} \quad (44)$$

where \bar{Y} is a $2N \times 2N$ matrix:

$$\bar{Y} = \begin{bmatrix} \bar{Y}^{uu} & -\bar{Y}^{ub} \\ -\bar{Y}^{bu} & \bar{Y}^{bb} \end{bmatrix} = \begin{bmatrix} \bar{Y}^{uu} & -\bar{Y}^{ub} \\ -\bar{Y}^{ub} & \bar{Y}^{uu} \end{bmatrix}. \quad (45)$$

6.1. The Combined Interior and Exterior Problem and Scattering Matrix. For a single via labeled as via 1 (Fig. 4), the exterior problem for $z > d/2$ has a magnetic current opposite that of the interior problem, with the same voltage:

$$\bar{M}_s^{(e)}(\bar{\rho}') = \frac{V_{1u}}{|\bar{\rho}' - \bar{\rho}_1| \ln(b/a)} \hat{\phi}_{\rho\rho_1}^t, \quad \text{for } a \leq |\bar{\rho}' - \bar{\rho}_1| \leq b. \quad (46)$$

Defining the current I_{1u} and I_{1b} as flowing out of the slab, then we have

$$\begin{bmatrix} B_{1u} \\ I_{1u} \end{bmatrix} = \begin{bmatrix} \Gamma_{sc,1u} & T_{ant,1u} \\ I_{sc,1u} & Y_{ant,1u} \end{bmatrix} \begin{bmatrix} A_{1u} \\ -V_{1u} \end{bmatrix}. \quad (47)$$

For the exterior problem of the lower port, we have a magnetic current opposite the interior problem. To maintain the same matrix form of Eq. (47), the current will be flowing out of the waveguide slab, and is equal to $-I_{1b}$:

$$\bar{M}_s^{(e)}(\bar{\rho}') = \frac{V_{1b}}{|\bar{\rho}' - \bar{\rho}_1| \ln(b/a)} \hat{\phi}_{\rho\rho_1}^t, \quad \text{for } a \leq |\bar{\rho}' - \bar{\rho}_1| \leq b \quad (48)$$

$$\begin{bmatrix} B_{1b} \\ -I_{1b} \end{bmatrix} = \begin{bmatrix} \Gamma_{sc,1b} & T_{ant,1b} \\ I_{sc,1b} & Y_{ant,1b} \end{bmatrix} \begin{bmatrix} A_{1b} \\ V_{1b} \end{bmatrix}. \quad (49)$$

The definitions are extended to N upper and lower ports. Define $N \times N$ diagonal matrices with $\bar{\Gamma}_{sc}^u, \bar{\Gamma}_{sc}^b, \bar{T}_{ant}^u, \bar{T}_{ant}^b, \bar{I}_{sc}^u, \bar{I}_{sc}^b, \bar{Y}_{ant}^u$, and \bar{Y}_{ant}^b and $N \times 1$ column matrices $\bar{A}^u, \bar{A}^b, \bar{B}^u, \bar{B}^b$.

Solving the combined problem of the exterior and interior problem gives a $2N \times 2N$ scattering matrix of \bar{S} :

$$\begin{bmatrix} \bar{B}^u \\ \bar{B}^b \end{bmatrix} = \bar{S} \begin{bmatrix} \bar{A}^u \\ \bar{A}^b \end{bmatrix} \quad (50)$$

$$\bar{S} = \begin{bmatrix} \bar{S}_{uu} & \bar{S}_{ub} \\ \bar{S}_{bu} & \bar{S}_{bb} \end{bmatrix}. \quad (51)$$

6.2. Simplified Exterior Problem with a Given Characteristic Admittance. We consider the simplified case of identical traces for the exterior problem with a given characteristic admittance Y_0 of the traces:

$$\begin{bmatrix} \bar{\Gamma}_{sc}^u & \bar{T}_{ant}^u \\ \bar{I}_{sc}^u & \bar{Y}_{ant}^u \end{bmatrix} = \begin{bmatrix} \bar{\Gamma}_{sc}^b & \bar{T}_{ant}^b \\ \bar{I}_{sc}^b & \bar{Y}_{ant}^b \end{bmatrix} = \begin{bmatrix} -\bar{1}_N & \bar{1}_N \\ -2Y_0 \bar{1}_N & Y_0 \bar{1}_N \end{bmatrix}. \quad (52)$$

Then the scattering matrix simplifies to

$$\bar{S} = \{Y_0 \bar{1}_{2N} + \bar{Y}\}^{-1} \{Y_0 \bar{1}_{2N} - \bar{Y}\} \quad (53)$$

where \bar{Y} is the admittance matrix of the interior problem as given by (45), and $\bar{1}_{2N}$ is the unit matrix of dimension $2N$.

For the case of two vias, the S -matrix is

$$\bar{S} = \begin{bmatrix} S_{1u1u} & S_{1u1b} & S_{1u2u} & S_{1u2b} \\ S_{1b1u} & S_{1b1b} & S_{1b2u} & S_{1b2b} \\ S_{2u1u} & S_{2u1b} & S_{2u2u} & S_{2u2b} \\ S_{2b1u} & S_{2b1b} & S_{2b2u} & S_{2b2b} \end{bmatrix}.$$

For the case of 256 vias, the S -matrix is of dimension 512×512 with two ports for each via.

6.3. Small Via Radius and Small Layer Thickness Approximations. For the case of a small via radius, we only keep

$$T_0^{\text{TM}} \text{ while all other } T_n^{\text{TM}} \text{ are discarded.}$$

Then only the $m = 0$ harmonics of the vias are coupled to each other, giving the Foldy–Lax equation of

$$w_{l_0}^{\text{TM}(q)} = a_{l_0}^{\text{TM}(q)} + \sum_{\substack{p=1 \\ p \neq q}}^N H_0^{(2)}(k_{\rho l} |\bar{\rho}_p - \bar{\rho}_q|) T_0^{(N)} w_{l_0}^{\text{TM}(p)}. \quad (54)$$

Then the dimension of the Foldy–Lax equation becomes only N .

After the Foldy–Lax equation above is solved, then the other azimuthal harmonic, if needed, can be calculated by using the Foldy–Lax equation for $n \neq 0$.

Since the currents are only dependent on $w_{l_0}^{\text{TM}(p)}$ and not on another harmonic, it is not necessary to calculate the other harmonic $w_{l_n}^{\text{TM}(p)}$. Next, we assume that the thickness of the slab is small, so only the finite number of modes up to l_{max} mode propagates from one cylinder to the other. This means that

$$H_0^{(2)}(k_{\rho l} |\bar{\rho}_p - \bar{\rho}_q|) = 0, \quad \text{for } p \neq q \text{ and } l > l_{\text{max}} \quad (55)$$

$$\bar{F}_l = \bar{I}_N, \quad \text{for } l_{\text{max}} < l < L_{\text{max}}. \quad (56)$$

When only the TEM mode is propagating, $l_{\text{max}} = 0$. Then the Foldy–Lax equation needs only to be solved for the TEM mode. However, other modes $l \neq 0$ do contribute to the direct terms in near-field interaction as given by the incident field coefficient in Eq. (25). We have, using (56) in (35),

$$\bar{Y}^{uu} = B_0 \bar{P}_0 + \sum_{l \neq 0} B_l \bar{E}_l \quad (57)$$

$$\bar{Y}^{bu} = D_0 \bar{P}_0 + \sum_{l \neq 0} D_l \bar{E}_l \quad (58)$$

where \bar{E}_l for $l > 0$ is a diagonal matrix as a result of (32) and (33) when only the $l = 0$ mode propagates.

7. NUMERICAL RESULTS AND DISCUSSION

Figure 5 shows the scattering parameters of two adjacent coupled vertical vias without surrounding passive vias. The purpose of this simulation for only two coupled vias is to validate the Foldy–Lax approach for via coupling. A comparison was made between the Foldy–Lax approach and the approach used in [6]. The simulation of the exterior structure has been totally separated from the simulation of the interior structure. In producing the result in Figure 5, for the sake of comparison, we use the same coaxial cable feed in and the

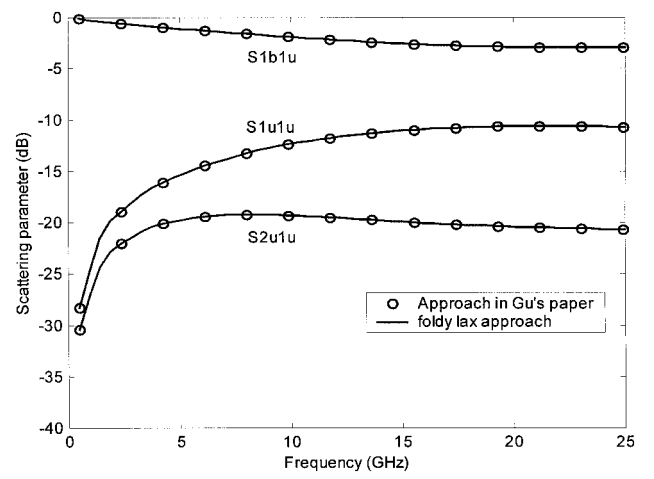


Figure 5 Scattering parameter of two coupled vertical vias. Comparison with [6]

same parameters as in [6], which are: the inner radius of the via is $a = 0.457$ mm, the outer radius of the via is $b = 1.524$ mm, the separation of the two vias is $s = 4$ mm, and the layer thickness is $d = 1.524$ mm, with a layer relative dielectric constant of $\epsilon_r = 2.2$. The result shows good agreement for two via couplings. The simulation was made for single layer due to the fact that the result can be easily extended to the multilayer case using a cascade of transfer matrices [6].

Figure 6 shows the scattering parameters of two adjacent coupled vertical vias in the vicinity of 254 other vias. A comparison was made between the Foldy–Lax approach, which considers the multiple scattering from those other 254 vias, and the approach in [6]. The positions of the 256 vias are generated randomly, with a fractional volume of 2%. The geometry of the positions of these 256 vias is shown in Figure 7, where the scattering parameters of the two circled vias are calculated. Out of the 512×512 scattering matrix, we only show the S -parameters (S_{1u1u} , S_{1b1u} , and S_{2u1u}) of the two active vias. The results shows clearly that, due to the multiple scattering of a large number of adjacent vias, although the transmission remains almost the same, the coupling between two vias can be severely affected. The curve for the coupling

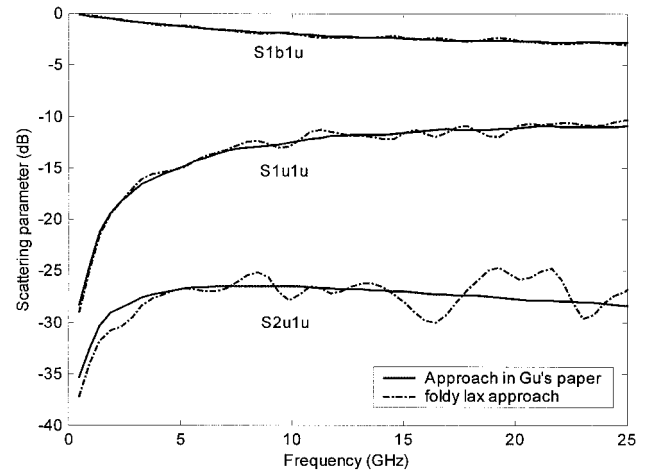


Figure 6 Scattering parameter of two coupled vertical vias in the vicinity of 254 other vias. Comparison with coupled via model when effects of the other 254 vias are ignored

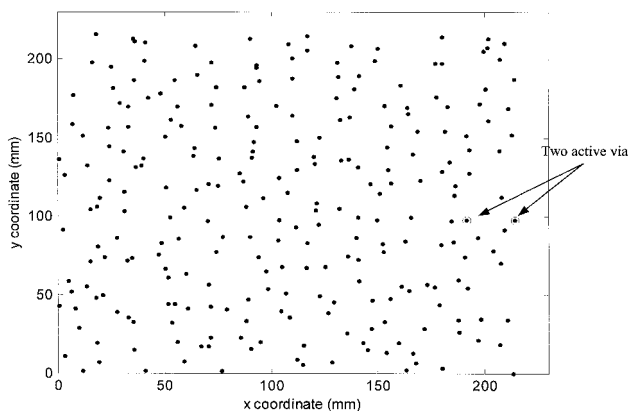


Figure 7 Geometry distribution of 256 randomly distributed vias, with the two active vias indicated; other 254 vias are idle

coefficient in Figure 6 has a random multiple ripple because of the random distribution and multiple scattering from other via cylinders.

For massively coupled vertical vias, compared with the pure numerical method, a simulation using the Foldy–Lax multiple scattering equations greatly improves the computational speed, while reserving the accuracy because of its semianalytical characteristics. On the other hand, compared with the analytical approach which only takes into account two via couplings, the Foldy–Lax formulation improves the accuracy by considering the influence of multiple scattering from other adjacent vias. This is important, especially for the calculation of the coupling effect. As shown in the numerical result, the coupling between two vias can be quite different when considering the influence of a large number of adjacent vias. Considering the ever-increasing density of via discontinuity in electronic packaging, this approach can find applications in areas like electronic design automation, and can help engineers in designs for signal integrity.

REFERENCES

1. T. Wang, R.F. Harrington, and J.R. Mautz, Quasi-static analysis of a microstrip via through a hole in a ground plane, *IEEE Trans Microwave Theory Tech* 36 (1988), 1008–1013.
2. S.-G. Hsu and R.-B. Wu, Full wave characterization of a through hole via using the matrix-penciled moment method, *IEEE Trans Microwave Theory Tech* 42 (1994), 1540–1547.
3. S.-G. Hsu and R.-B. Wu, Full-wave characterization of a through hole via in multi-layered packaging, *IEEE Trans Microwave Theory Tech* 42 (1994), 1073–1081.
4. B. Archambeault, C. Brench, and O.M. Ramahi, *EMI/EMC computational modeling handbook*, Kluwer Academic, Norwell, MA, 1998.
5. Q. Gu, Y.E. Yang, and M.A. Tassoudji, Modeling and analysis of vias in multilayered integrated circuits, *IEEE Trans Microwave Theory Tech* 41 (1993), 206–214.
6. Q. Gu, A. Tassoudji, S.Y. Poh, R.T. Shin, and J.A. Kong, Coupled noise analysis for adjacent vias in multilayered digital circuits, *IEEE Trans Circuits Syst* 41 (1994), 796–804.
7. D.V. Otto, The admittance of cylindrical antennas driven from a coaxial line, *Radio Sci* 2 (1967), 1031–1042.
8. L. Tsang, J.A. Kong, and R.T. Shin, *Theory of microwave remote sensing*, Wiley Interscience, New York, 1985.
9. L. Tsang, J.A. Kong, and K.H. Ding, *Scattering of electromagnetic waves: Vol. 1, Theory and applications*, Wiley Interscience, New York, 2000.

10. L. Tsang, J.A. Kong, K.H. Ding, and C. Ao, *Scattering of electromagnetic waves: Vol. 2, Numerical simulations*, Wiley Interscience, New York, 2001.

© 2001 John Wiley & Sons, Inc.

DESIGN OF NARROWBAND AMPLIFIERS WITH CONDITIONALLY STABLE TRANSISTORS

Dario Benvenuti,¹ Maurizio Cicolani,¹ Stefano Pisa,² Pasquale Tommasino,² and Alessandro Trifiletti²

¹ Alenia Marconi Systems

00131 Rome, Italy

² Department of Electronic Engineering

University "La Sapienza" of Rome

00184 Rome, Italy

Received 24 May 2001

ABSTRACT: A technique to design narrowband amplifiers by using conditionally stable transistors is presented. The proposed analytical approach allows us to design lossless matching networks, by providing power matching at one port and minimum mismatch at the other port. The use of this technique leads to high gain as well as proper stability margins. © 2001 John Wiley & Sons, Inc. *Microwave Opt Technol Lett* 31: 208–210, 2001.

Key words: narrowband amplifiers; conditional stability; optimal return loss

1. INTRODUCTION

The design of microwave and millimeter-wave amplifiers is carried out, taking into account stability requirements as well as circuit performance. The fulfillment of the unconditional stability criterion (i.e., Rollett stability factor K greater than 1 and modulus of the scattering matrix determinant lower than 1, or other equivalent formulations [1], for a single-stage amplifier) allows us to choose the termination load and source impedances on the Smith chart with no constraints, and to achieve the desired performance in terms of gain (in particular, the maximum available gain), return loss, and noise figure.

For conditional stable transistors (i.e., with $|K| < 1$), design techniques such as resistive loading [2–4] are used to provide stabilization of the devices; however, the use of resistors, which also permits good matching and flat gain over a wide band, produces a noise figure increase and gain reduction. This drawback can be avoided by using lossless matching networks, as in [5–6] where an approach to design a narrowband single-sided matched amplifier by using conditionally stable devices with $0 < K < 1$ was proposed. This approach allows the stabilization of devices without introducing lossy matching networks, and permits us to obtain perfect matching at one port and maximum transducer gain compatible with this condition. However, a high return loss is usually obtained at the mismatched port. An iterative approach is typically used to determine the optimal loading conditions which minimize the mismatch.

In this paper, we present the results of an analytical approach that permits the calculation of minimum mismatch in terms of the K -factor, and to set design goals for the lossless matching network.